LAWRENCE
LIVERMORE
NATIONAL
LABORATORY

LLNL-CONF-654599

Value of MT inversions for geothermal exploration: accounting for multiple interpretations of field data & determining new drilling locations

W. Trainor-Guitton, G. M. Hoversten, G. Nordquist, R. Intani, R. Mellors, J. Roberts

May 19, 2014

World Geothermal Congress 2015
Melbourne, Australia
April 19, 2015 through April 25, 2015

Disclaimer

Proceedings World Geothermal Congress 2015
Melbourne, Australia, 19-25 April 2015

Value of MT inversions for geothermal exploration: accounting for multiple interpretations of field data & determining new drilling locations

Whitney J. Trainor-Guitton[1], G. Michael Hoversten[2], Gregg Nordquist[3], Rindu Grahabhakti Intani[4], Robert Mellors[1], and Jeffery Roberts[1]

[1]Lawrence Livermore National Laboratory, 7000 East Avenue

trainorguitton@llnl.gov

[2]Chevron Energy Technology Company, San Ramon, CA

[3]Chevron Geothermal Services Company, Makati City, Philippines

[4]Chevron Geothermal Power Indonesia, Jakarta, Indonesia

Keywords: value of information, resource assessment, magnetotellurics

ABSTRACT

How well does geophysical data improve our geothermal prospecting decisions? How much is this information worth? These types of questions can be answered using the value of information (VOI) method. VOI quantifies how relevant any particular information source is, given a decision with an uncertain outcome; thus, the estimated VOI can be used to justify the purchase of additional data when exploring for geothermal resources. Previously, a value of information (VOI) methodology using synthetic data for the exploration geothermal problem was presented (Trainor-Guitton et al., 2013a; 2013b). Evaluating the reliability of geophysical method to decipher key spatial subsurface features is relatively straightforward with synthetic data since many different "true" subsurface models can be tested.

Perhaps a more useful analysis is to decipher the reliability of field data that has been "calibrated," e.g. production parameters have been observed that are approximately collocated with the geophysical data. Specifically, we consider a 3D electrical resistivity model that has been constructed from MT (magnetotellurics) data via geophysical inversion. We are especially interested in how multiple interpretations of the inversion model can be incorporated into the reliability analysis. Typically, MT data are used to detect the electrically conductive clay cap which can be indicative of geothermal alteration occurring just above the resource. Several interpretations of the clay cap (a 3D feature) are possible and may result in different estimates of the effectiveness of the MT technique to detect electrically conductive targets that can be indicative of potential geothermal resources, representative of the well data (steam flow, permeability and pressure). We will present several alternative interpretations that will highlight the challenges and advantages of using field data to estimate the value of geophysical information. Our results, however, indicate that the final VOI estimate was not strongly dependent on the different interpretations of the same MT inversion model. Additionally, we demonstrate how these VOI evaluations can be used to guide future drilling locations.

1. INTRODUCTION

The value of information (VOI) quantifies how relevant and reliable any particular information source is, and quantifies its value when making a decision with an uncertain outcome. VOI can be used to justify the costs of collecting and processing the planned data. It has been used in oil exploration (see review by Bratvold et al., 2009). We apply it here to geophysical data from a geothermal field. Previous work (Trainor-Guitton et al., 2013a,b) tested the applicability for geothermal exploration using synthetic datasets.

VOI is method from the field of decision analysis. Decision analysis concepts are often described in terms of lotteries and prizes (Pratt et al., 1995). By choosing to drill or not, a decision maker is choosing whether or not to participate in a lottery with certain perceived chances of winning a prize (drilling into a profitable reservoir); however, this lottery also involves the chances of losing money (drilling into an uneconomic reservoir). VOI estimates the possible increase in expected utility (winning a lottery with a bigger prize) by gathering information before making a decision, such as where or if to drill a production well. In its simplest form, the VOI equation can be expressed as:

$$VOI = V_{with\ information} - V_{prior} \tag{1}$$

where V is the value, the metric used to quantify the outcome of a decision. The higher the value, the more "successful" an outcome of a decision is. Therefore, value is the revenue gained minus the costs incurred for any particular decision action taken. The simplest representation of the decision in geothermal exploration is "to drill or not" for one particular location; if heat, permeability and fluids exist in that location, then the value outcome of that decision will be high. Otherwise, the value outcome will be a monetary loss.

We consider how well the clay cap, as delineated by a 3D MT data inversion, can indicate magnitude of the steam flow by utilizing a dataset from an operating geothermal field. The electrically conductive materials imaged by MT are created by geochemical alteration when hot fluids circulate within subsurface geologic units (Gunderson et al., 2000). However, if the hot fluid source ceases to exist, the electrically conductive material will remain, thus a clay cap does not guarantee current geothermal activity (Karlsdóttir et al., 2012).

The contributions presented in this paper are twofold. First, our work illustrates the implementation of a VOI methodology given the uncertainties of geothermal exploration and multiple interpretations of the clay cap from a 3D MT inversion. We utilize an existing dataset of steam flow measurements to deduce trends between steam flow and electrical conductivity, thereby using the past performance of the geophysical technique to predict steam flow. The VOI's produced can be used to determine if MT should be collected again in a field with similar geological and geophysical attributes. The second set of results presented here demonstrate how the VOI evaluations can serve as a guide on deciding where to drill for new production wells in undeveloped areas given that the MT information has already been collected in that area.

The paper is organized as follows. First the steam flow and MT data sets are described. Then we describe how the 3D cube of electrical conductivity is used to infer the location and margins of the clay cap: the potential margins or boundaries of the geothermal reservoir. Third, we will describe the different set of assumptions used to determine the different clay caps and the colocation between the electrical conductivity of the clay cap and a steam flow measurement. The various conductivity and spatial thresholds produce various interpretations of the "calibrated dataset." Fourth, these multiple interpretations will provide three estimates of the MT's reliability to delineate the boundaries of the geothermal reservoir. Finally, we will use these reliabilities to 1) calculate VOI's (values of information) of MT and 2) provide guidance on where future drilling should be focused.

1.1 Darajat geothermal field

Darajat is vapor geothermal field located in West Java, Indonesia. It is located about 150 km to the southeast of Jakarta and has an elevation ranging from 1,750 to 2,000 meters above sea level. First production from the field was started in 1994 with installation of a 55 MW plant. Additional capacity was added in 2000 and 2007 to bring the total production capacity to 271 MW from three power plants.

The Darajat geothermal field is located along a range of Quaternary volcanic centers in West Java. It is spatially associated with an eroded andesitic stratovolcano, Gunung Kendang. The reservoir is dominantly comprised of thick lava flows and intrusions in a stratovolcano central facies, with relatively higher porosity, thick pyroclastic sequences of proximal to medial facies that were deposited more toward the margins. Structures trend predominantly NE-SW but also include N-S and NW-SE trending faults (Rejeki et al., 2010).

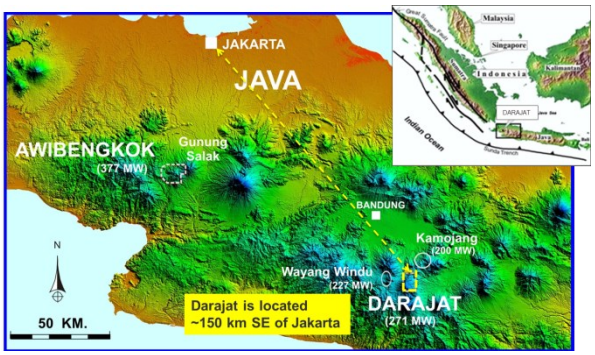

Figure 1: Location of the Darajat geothermal field in West Java

1.2 Data sets used in this study

1.2.1 Steam flow measurements

The steam flow dataset contains the average production over one year for 23 different wells. The steam flow data approximately spans an area of 2.6 km by 4.2 km and a depth range of 600m to 1800m below the surface. Figure 2 displays a histogram of these steam flow measurements. The steam flow measurements are composite flows for all feed zones from each well.

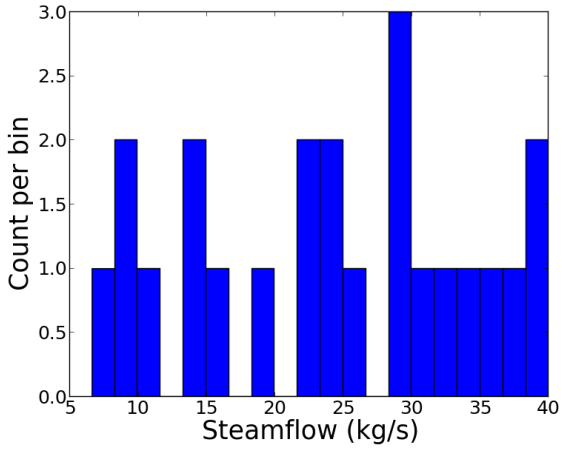

Figure 2: Histogram of steam flow data from 23 wells.

For this VOI demonstration, we categorized the *steam flow magnitude into* seven groups or bins, represented by θ_i:

$$\theta_i \; i \in \begin{cases} 7, & \theta \geq 30\ kg/s \\ 6 & 25 \leq \theta < 30\ \text{kg/s} \\ 5' & 20 \leq \theta < 25\ \text{kg/s} \\ 4, & 15 \leq \theta < 20\ \text{kg/s} \\ 3, & 10 \leq \theta < 15\ \text{kg/s} \\ 2, & 5 \leq \theta < 10\ \text{kg/s} \\ 1, & 0 \leq \theta < 5\ \text{kg/s} \end{cases} \quad (2)$$

We define our prior uncertainty with respect to steam flow production using these steam flow categories. Let us represent this by

$$\boldsymbol{z}(\theta_i) \;\; i = 1, \ldots, 7, \quad (3)$$

where vector $\boldsymbol{z}$ represents the non-dimensional steam flow categories that may be realized from production wells. Future work will incorporate spatial aspects of this steam flow possibility. The steam flow categories can be used to represent the economic (value) outcome of a drilling decision at any location (*x,y,z*).

1.2.2 Magnetotellurics

The MT data used for this analysis consists of 85 remote referenced stations which were distributed over and outside the boundaries of the Darajat geothermal field. The data were collected in 1996-97 and 2004 and were used to interpret the distribution and extensions of the electrically conductive clay cap beyond the first development area (Rejeki et al., 2010). The off-diagonal impedances between 100 seconds and 100 Hertz were inverted using the 3D algorithm of Newman and Alumbaugh (2000). The impedance errors derived from the multi-station robust processing were used subject to a 10% error floor. The starting model was a 10 Ω-m halfspace beneath the topography. The inversion reduced the RMS data misfit from 87 to 1.3.

2. METHODOLOGY

Our methodology estimates the prediction power of MT given a collocated steam flow dataset. First, we consider the decision of "to drill or not," and we make two evaluations of the efficacy of MT via several interpretations of the MT inversion model. It is possible to extend the methodology to the more complex decision of "where to drill." We assume that the decision outcome only depends on the possible steam flow of a reservoir.

2.1 Interpretations of clay cap: different conductivity thresholds *only*

We have one 3D model of conductivity inverted from the MT dataset described above which overlies where the steam flow measurements were made. First, we use only this inversion model to determine possible relationships between the electrical conductivity property and the steam flow magnitude. Typically, the high conductivity layer can be used to estimate the likely margins of the geothermal system (Cumming, 2009). We attempt to assess whether the thickness and conductivity information of the clay cap can be used to distinguish between higher and lower steam flow.

As we assume that the "clay cap" margins can be used to infer the boundaries of the geothermal resource, we define a conductivity threshold in order to delineate the location and thickness of the clay cap. We use a bottom threshold value of σ=0.12 S/m. Thus, a top and bottom surface is defined where the electrical conductivity begins to decrease from the threshold value of σ=0.12 S/m. The resulting cap is pictured in Figure 3.

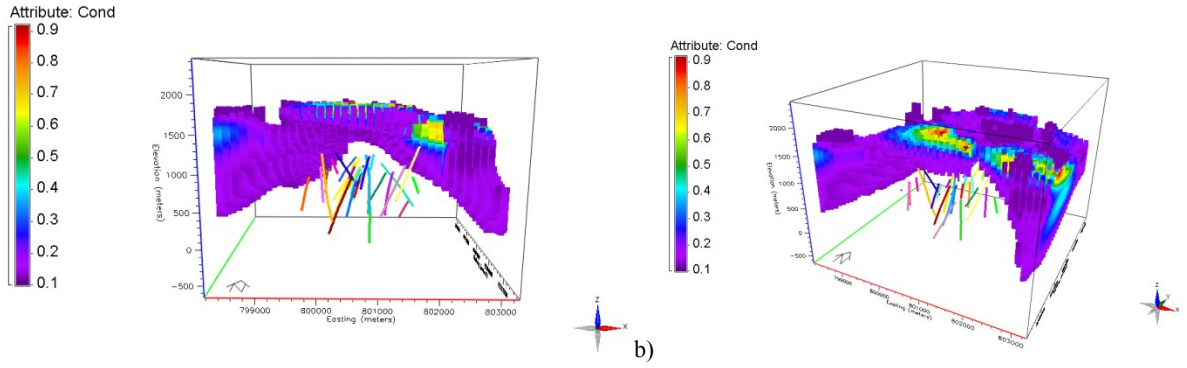

a) b)

Figure 3: a) Cross sectional view and b) top view of clay, defined by threshold σ=0.12 S/m. Wells containing steam flow measurements shown in multicolor.

2.1.1 Defining "collocated" electrical conductivity and steam flow

Next, we determine which conductivity locations within the clay cap that can be correlated with the steam flow measurements. We suggest that steam flow measurements closer to the cap are more likely influence the electrical conductivities and geometry of the clay cap. Therefore, we expect a stronger relationship between the steam flow measurements that are closer to the clay cap.

We begin by defining 625m as the maximum distance between a steam flow measurement and any point within the clay cap. We choose this distance because it represents the lower quartile of all distances between the clay cap conductivities and steam flow locations. Figure 4a) displays the midpoint of Well 15 as a brown box along the well path (red) and the conductivity values of the clay cap. First, the location of the closest conductivity measurement to the well midpoint is determined. Then, the neighboring

conductivity values in the clay cap are averaged within a radius of 100 m to compare to the steam flow of that well. Figure 4b) displays only the conductivities measurements that are within 100m of the closest conductivity point for Well 15.

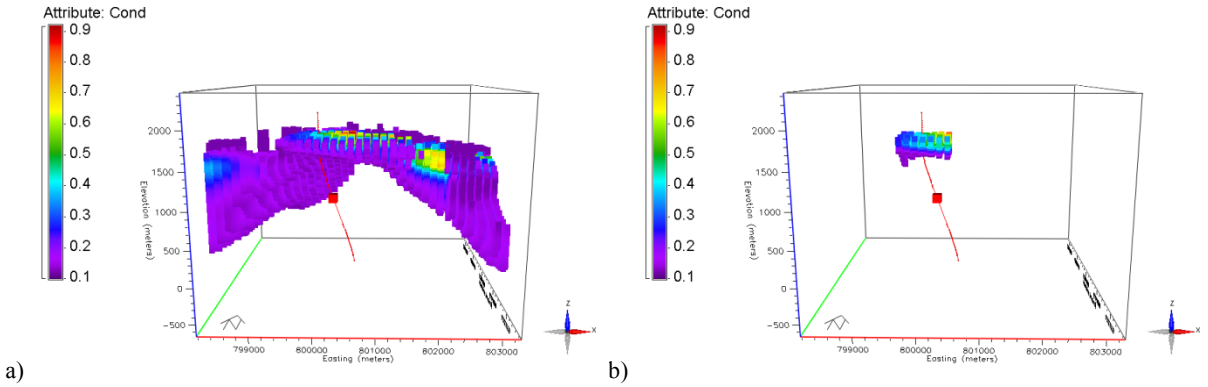

Figure 4: a) Well 15 midpoint (red box along red path) with conductivities of clay cap. b) Only the conductivities within 100m of the closest conductivity point to Well 15's midpoint.

This is repeated for any steam flow-clay cap pair that are less than 625m away. Figure 5a plots the geometric average of these neighboring conductivities versus the nearest steam flow measurement. Six of the 23 steam flow measurements locations were within the maximum threshold of 625m. Of this set, the conductivities show a slight positive correlation (0.28) with steam flow.

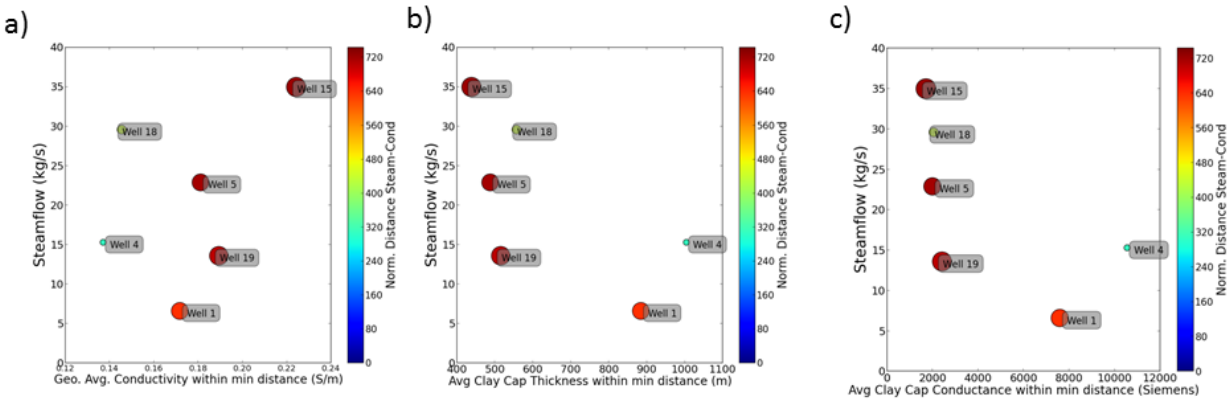

Figure 5: 2D scatterplot of co-located a) electrical conductivities (geometric average) b) thicknesses (arithmetic average) and c) conductance (all from 0.12S/m clay cap) and steam flow (maximum distance 625m). The size of the symbols reflects number of conductivities used in the average calculation and the color represents the distance

This same process is done for the clay cap thickness at these neighboring locations. Figure 5b displays the arithmetic average of the clay cap thickness versus the 6 steam flow measurements, and Figure 5c displays average conductance (the product of conductivity and clay cap thickness). Unlike Figure 5a, these two plots now show a relatively strong negative correlation with steam flow: -0.67 and -0.73 respectively. The negative correlation of steam flow with conductance (which is dominated by the thickness) is expected since greater temperatures (>200˚C) will alter the highly conductive smectite clays into more resistive illitic or chloritic clays (Ussher et al., 2000). The clay cap for this analysis is defined on the basis of conductivity and therefore is expected to dominantly represent the distribution of smectite. Since places that have been altered to illite will have lower conductivity they tend not be included in the clay cap interpretation as used in this analysis. Thus, if the interpreted clay cap based on the MT data is capturing only the higher conductive smectite, **one would expect a shallower base and a thinning of the clay cap over areas where the permeability is higher**. Therefore, we only consider and include the conductance (not conductivity or thickness alone) for the next two interpretations of clay cap for comparison with the steam flow measurements.

Next, we tested how sensitive these results are to the threshold which defines the clay cap. We now define the clay cap with the threshold of 0.1 S/m. This clay cap, shown in Figure 6, is slightly thicker than the clay cap defined by the threshold of 0.12 S/m (Figure 3).

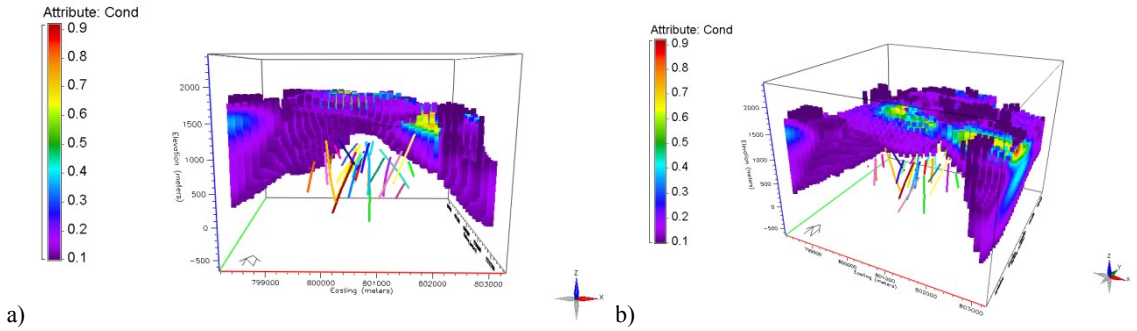

Figure 6: Cross sectional view of clay cap defined by threshold σ=0.10 S/m. Wells containing steam flow measurements shown in multicolor.

This thicker clay cap produces more pairs of steam flow/conductivity location pairs when using the maximum distance of 625m. Figure 7 only plots the eight steam flow measurements versus their neighboring conductance, since this relationship may be more revealing of reservoir temperature. The resulting correlation coefficient is -0.7.

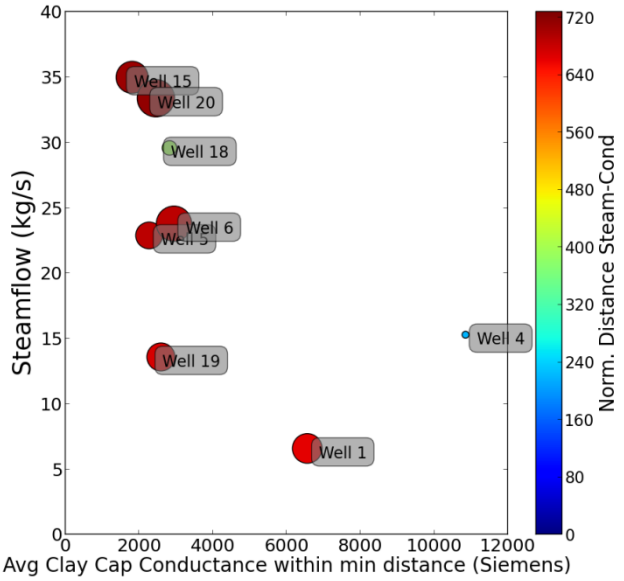

Figure 7: 2D scatterplot of co-located conductance (from 0.10S/m clay cap) and steam flow (maximum distance 625m). The size of the symbols reflects number of conductivities used to calculate the average and the color represents the distance

2.3 Establishing estimations of the data reliability/likelihood: How well does the conductance of the clay cap distinguish the steam flow categories?

As described in the Introduction, a data reliability or likelihood is necessary to evaluate VOI. The reliability quantifies the uncertainty in the relationship between the electrical conductance and the steam flow magnitude. We have two interpretations of the clay cap from the 3D MT inversion. In order to have sufficient measurements to compute some statistics for the data reliability, we will use all conductivity measurements used to calculate the geometric means of conductance on the x-axes of Figure 5c and Figure 7. Figure 8 and Figure 9 depict the counts of every conductance measurement from Figure 5c and Figure 7: the clay cap defined by a threshold of 0.12 S/m and 0.10 S/m. The counts in the histograms are represented by c_{ij}, where c is the total number of measurements that fall within conductance bin *j* and are associated with one of the seven steam flow categories *i* (Equation 2).

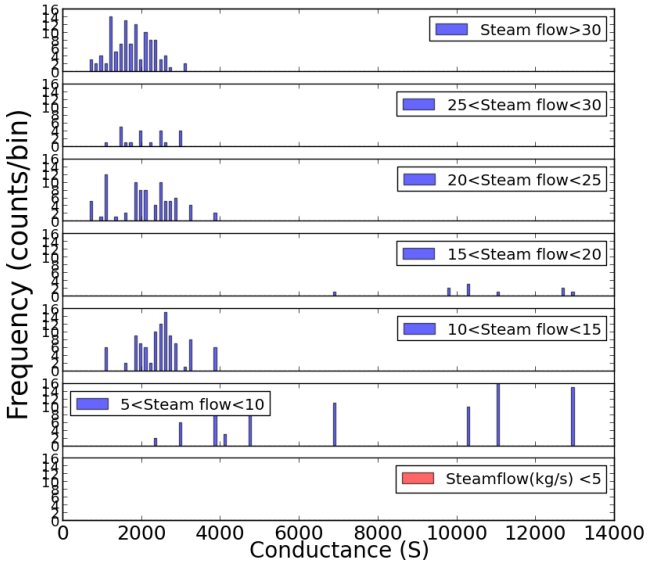

Figure 8: From clay cap defined by 0.12 S/m : counts (blue bars) of conductance measurements in bin j (horizontal axis) that correspond to steam flow bin i (different vertical rows).

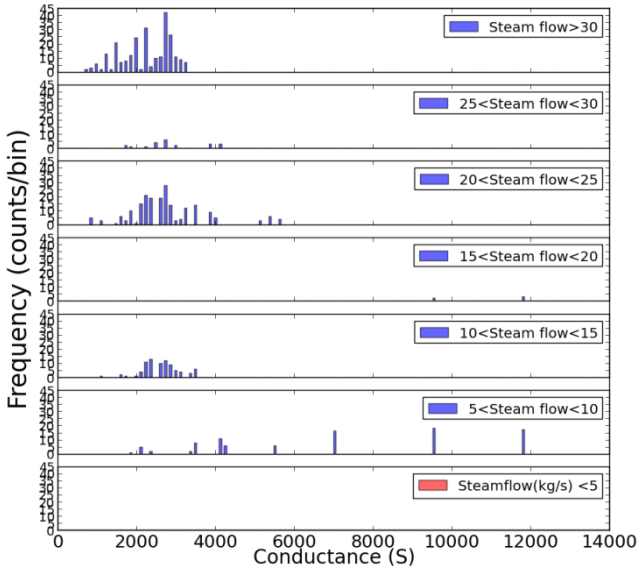

Figure 9: From clay cap defined by a) 0.10 S/m: counts (blue bars) of conductance measurements in bin j (horizontal axis) that correspond to steam flow bin i (different vertical rows).

The data likelihood (which is also the reliability) considers how likely a conductance bin is given that we know the steam flow categories (θ_i) associated with it. Therefore, the counts in bin *ij* are normalized by total number of measurements in that steam flow category (*i*):

$$Pr(G = g_j|\Theta = \theta_i) = \frac{c_{ij}}{\sum_i c_{ij}} \qquad (4)$$

$$i = \{1,2,3,4,5,6,7\}\, j = 1, \dots, J$$

where the electrical conductance is represented by g. The denominator, $\sum_i c_{ij}$, represents normalization by the sum of all data points within that steam flow category (*i*).

Next, we want to establish the information posterior which establishes a "misinterpretation rate" or how uniquely a conductance bin can distinguish between any of the steam flow categories θ_i. According to Bayes law, the posterior is equal to the product of the prior probability and the likelihood scaled by the marginal

$$Pr(\Theta = \theta_i | G = g_j) = \frac{Pr(\Theta = \theta_i) Pr(G = g_j | \Theta = \theta_i)}{\sum_{k=1}^{N+1} Pr(\Theta = \theta_k) Pr(G = g_j | \Theta = \theta_k)} = \frac{Pr(\Theta = \theta_i) Pr(G = g_j | \Theta = \theta_i)}{Pr(G = g_j)} \quad i = \{1,2,3,4,5,6,7\}\, j = 1, \dots, J \tag{5}$$

The corresponding posteriors of the different counts in Figure 8 and Figure 9 are the solid colored lines in Figure 10 and Figure 11. Figure 10 and Figure 11 only plot to a maximum 6,000S since most of the conductance measures of the clay caps are less than this and it allows for easier viewing. The colors of the bars will be explained in Section 3.3. When the posterior is close to 1 or 0 (right hand y-axis label), this indicates that the data in that conductance bin is more informative.

Visually, the red posterior (steam flow > 30 kg/s) from the clay cap defined by only the 0.12 S/m threshold (top of Figure 10) has a high posterior (~1) value for the conductance bins <1,200S. This will contribute to a higher VOI evaluation. The posterior for 25<θ<30 for the 0.10Sm clay cap is similar: consistently high for conductance bins <1,500S.

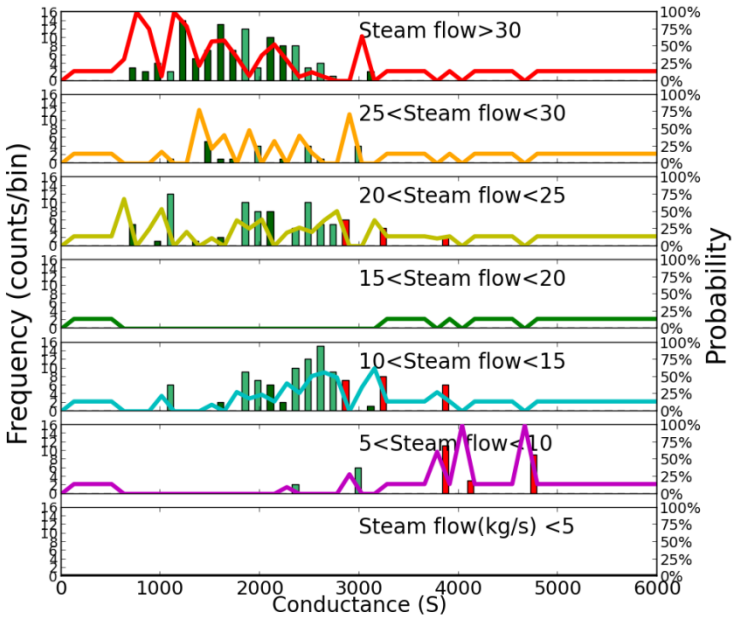

Figure 10: Counts (blue bars) and posteriors (solid lines) for the clay cap interpretations defined at 0.12 S/m. The sum of the posterior across the steam flow categories equals 100%.

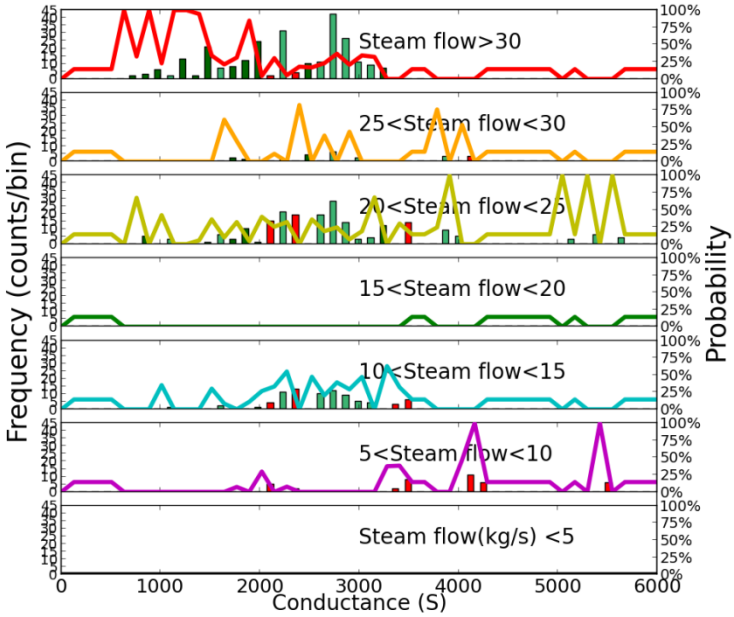

Figure 11: Counts (blue bars) and posteriors (solid lines) for clay cap interpretation defined at 0.10S/m. The sum of the posterior across the steam flow categories equals 100%.

3. VOI CALCULATION: DESCRIPTION & RESULTS

This section describes the calculations necessary to estimate the value of imperfect information using the information posteriors plotted in Figure 10 and Figure 11. First, the V_{prior} or the prior value is described.

3.1 V_{prior}: the best decision option given prior uncertainty

We will now describe how each prior model is linked to possible economic outcomes. This will be summarized in the quantity V_{prior}, which translates our prior uncertainty (our current state of information) into an expected (or average) outcome from our decision.

Recall that decision analysis frames the decision as the chance to enter the geothermal lottery with perceived chances of winning a prize (e.g. drilling into a profitable reservoir). By utilizing V_{prior}, a decision-maker can logically determine when one should participate in this lottery given both the prior uncertainties and possible gains and losses. The value metric allows for comparison between outcomes from different decision alternatives, which can be represented by function d_a.

$$v_a^{(t)}(\theta_i) = d_a\left(\boldsymbol{z}(\Theta = \theta_i)^{(t)}\right) \qquad (6)$$

$$a = 1{,}2 \quad i = 1, \ldots, 7 \quad t = 1, .. T$$

We assume only 2 possible alternatives (a = 1 or 2): drill/produce the reservoir or do nothing. Table 1 defines the 14 possible outcomes, which is a result of these 2 decision alternatives and the 7 possible reservoir categories. The columns represent the decision alternatives (a=1 and a=2) and the rows the different steam flow categories (θ_i).

Table 1: Table of nominal value outcomes for the 2 possible decision options (columns) and 5 possible economic viability categories of the unknown subsurface (rows).

Decision option→ ↓Steam Flow Rate (kg/s)	$v_{a=1}^{(t)}(\theta_i)$ a = 1 (drill under cap)	$v_{a=2}^{(t)}(\theta_i)$ a = 2 (do nothing)
$30 \leq \theta_i$	$700,000	$0
$25 \leq \theta_i \leq 30$	$300,000	$0
$20 \leq \theta_i \leq 25$	$125,00	$0
$15 \leq \theta_i \leq 20$	$40,000	$0
$10 \leq \theta_i \leq 15$	$0	$0
$5 \leq \theta_i \leq 10$	-$200,000	$0
$\theta_i \leq 5$	-$500,000	$0

Table 1 represents hypothetical, monetary values that could represent relative gains (payouts-- shown in black-- when you drill a well with economic production rates) or losses (loss on investment –shown in red--when you drill an uneconomic well). Specific

(and more realistic) gains and losses for a particular field site can be easily substituted in Table 1 and into the methodology. This would be necessary to use the resulting VOI's to determine if a particular data type is worth purchasing at a specific field site. The values in Table 1 are simply for demonstration purposes so that the behavior of the VOI quantities can be visualized.

All the necessary quantities have been introduced to calculate V_{prior}.

$$V_{prior} = \max_a \left(\sum_{i=1}^{7} Pr(\Theta = \theta_i) v_a(\theta_i) \right) \quad (7)$$

$$a = 1,2$$

In words, V_{prior} quantifies the best the decision-makers can do with the current uncertainty (no MT data has been collected), which are reflected in the prior probabilities $Pr(\Theta = \theta_i)$. V_{prior} identifies which decision alternative gives *on average* the best outcome (done through the $\max_a$). When considering a specific location for geothermal exploration, these prior probabilities should come from a geologist and/or other experts with knowledge of the geologic structure and history. For now, we assume $Pr(\Theta = \theta_1) = 40\%$ (steam flow < 5 kg/s) and all other categories $Pr(\Theta = \theta_i) = 10\%$ $i = 2,..,7$. These can be changed and the final VOI will depend on these prior probabilities.

Returning to the lottery example, when V_{prior} is 0, the decision-maker should "not participate in the lottery" (i.e. don't drill) given the current state of information. V_{prior}=0 tells the decision-maker that the decision alternative to "do nothing" will yield the higher outcome on average. V_{prior}=0 reflects the potential for large losses when you "participate in the lottery" or drill to produce a geothermal reservoir. The decision-maker would only be wise to participate in the lottery when $V_{prior} > 0$. Given the assigned prior probabilities and the value outcomes of Table 1, V_{prior} =\$0 for this example.

3.1 $VOI_{perfect}$: Upper bound on the value of information

The value of perfect information can be calculated using Equation 1, by substituting in $V_{perfect}$ for the value with information ($V_{with\ information}$). $VOI_{perfect}$ assumes that an information source exists that will always identify the correct economic viability category θ_i without errors. Like V_{prior}, $V_{perfect}$ only depends on the prior uncertainty and potential gains/losses of the problem.

$$V_{perfect} = \sum_{i=1}^{7} Pr(\Theta = \theta_i) \left(\max_a v_a(\theta_i) \right) \quad (8)$$

Here, we see that for each steam flow rate category θ_i, we can choose the best decision alternative *a* (this is reflected in $\max_a$ being performed before the average). With perfect information, we always know when the reservoir is uneconomic, and therefore we will always choose not to participate in the lottery. Thus, we remove the chance of loss by collecting perfect information. With our current state of information, we would not enter the lottery when the potential losses were too high relative to the gains. But with a flawless information source to allow us to avoid these losses, we may choose to participate in the lottery. Since it assumes error-free information, the $VOI_{perfect}$ quantity will give an upper bound on what we could expect for any information source. For this example, using the values in Table 1, $V_{perfect}$ = \$116,500. Thus, since V_{prior} =\$0, $VOI_{perfect}$ = \$116,500.

3.2 $VOI_{imperfect}$ Results: Different Clay Cap Interpretations

Now we consider imperfect MT data and we estimate its reliability when distinguishing between the seven different possible steam flow categories θ_i. The data is from a specific location, and we are using it to generate the required information posterior, which influences VOI, but everything else (priors, value outcomes, etc.) is completely unrelated to the location and settings of the actual data set. The information posterior is the form actually used to calculate the value *with* imperfect information $V_{imperfect}$.

$$V_{imperfect} = \sum_{j=1}^{J} \Pr(G = g_j) \left\{ \max_a \left[\sum_{i=1}^{7} Pr(\Theta = \theta_i | G = g_j) v_a(\theta_i) \right] \right\} \quad (9)$$

Here, the posterior accounts for how often one may incorrectly infer a steam flow category given the inverted electrical conductance. The posterior is used to weigh the averaged outcome of each alternative and category combination $v_a(\theta_i)$. Since the decision is made after conductivity data has been collected, the best alternative ($\max_a$) is chosen given the interpreted category. Lastly, $V_{imperfect}$ is weighted by the marginal probability $\Pr(G = g_j)$, how often any of the particular inverted resistivities occur relative to other conductivity bins.

*Table 2: Table of **nominal** $V_{imperfect}$ and $VOI_{imperfect}$ for the 2 clay cap interpretations (rows).*

Clay Cap defined by threshold:	Max Dist Steam-Cap	$V_{imperfect}$	$VOI_{imperfect}$
0.12 Siemens/m	625m	\$111,871	\$111,871
0.10 Siemens/m	625m	\$107,515	\$107,515

Table 2 includes both the value with imperfect information ($V_{imperfect}$) and the value of imperfect information ($VOI_{imperfect}$). The value of imperfect information is calculated using Equation 1 where now the $V_{imperfect}$ is used in place of the generic term of $V_{imperfect}$. As expected, all the $VOI_{imperfect}$ estimates are lower than $VOI_{perfect}$ ($116,500). This demonstrates how the highest value outcome will not be realized because of the imperfectness of the data that can mislead the decision maker about the economic viability of the reservoir. **The two $VOI_{imperfect}$ results are not significantly different from each other.** The $VOI_{imperfect}$ assessed from the clay cap defined at 0.12S/m is slightly higher which can be explained by the posterior being ~1 for the highest steam flow category (Figure 10).

3.3 VOI for determining the next location to drill

The next set of results demonstrates how a VOI model covering the same volume as the MT inversion model can be constructed using the information posteriors and the decision outcomes (Table 1). Essentially, each conductance bin (j) can be assigned a value which is calculated in the inner two evaluations of Equation 9

$$v_j = \left\{ \max_a \left[\sum_{i=1}^{7} Pr(\Theta = \theta_i | G = g_j) v_a(\theta_i) \right] \right\} \quad (10)$$

The first evaluation is a weighted average of possible outcomes ($v_a(\theta_i)$) using the posterior as the weights. The next operation is the non-linear max, which identifies the best alternative given the possible misinterpretations possible for that conductance bin. Therefore, in the case where the posterior definitively (or nearly definitively) identifies the highest steam flow category (as in the case of Figure 10a), the v_j will be highest. But if no conductance range (bin) exists that exclusively (or close to exclusively) can identify the higher steam flow category, the v_j's will reflect this.

For this particular field, a future drilling campaign is considered in an area where the current MT inversion model covers, but no drilling has taken place and therefore, no existing steam flow information is available. We can plot the v_j's according to the MT inversion model and look specifically at the area under consideration for future drilling. This may guide future well locations by using the past performance of MT to locate high steam flow.

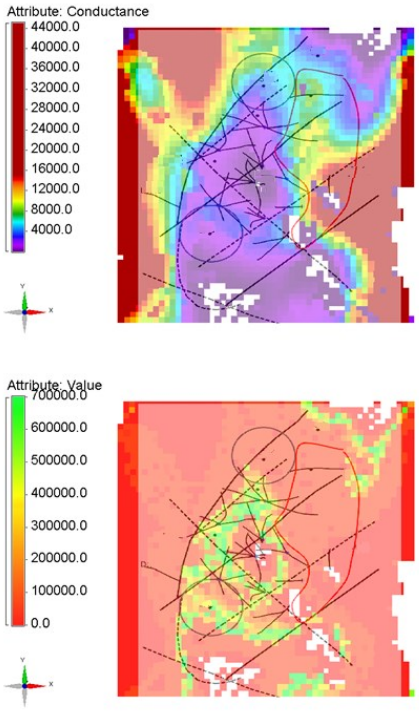

Figure 12: Plane View of field. Area within red solid line and the two black circles denotes location of possible future drilling campaign. a) conductance of clay cap interpreted with 0.12 S/m threshold b) resulting value ($) for each conductance bin (v_j) calculated using posterior in Figure 10.

Figure 12a displays the conductance (S) of the clay cap and Figure 12b displays the corresponding the conductance values in dollars (Equation 10) for the clay cap interpreted only with a 0.12S/m threshold. Overlain is the map of the field with surface traces of the faults (dashed black) and the area under consideration for future drilling (red solid line). Thus, by mapping back the value of each conductance bin, VOI provides some spatial guidance on where drilling will is most likely to produce a high valued result, given the past performance of MT. Figure 13 contains the conductance and value for the clay caps interpreted by the 0.10 S/m threshold.

Figure 12 and Figure 13 display very similar value patterns which makes sense since they differ by only a small conductivity cut-off. They display higher value outcomes around the existing two central wells, which could be described as a upside-down "V" green feature that follows the arching fault on the western boundary of the field. They also both have another East-West green (high value) feature intersecting the southern black circle which correlates with the ~800-900S feature. Recall, that the value is a function

of both the conductance bin's ability to exclusively identify a steam flow category (θ) and how economic that category is. Generally for these two calibrations, conductance bins <1,500S had the strongest relationship with the highest steam flow.

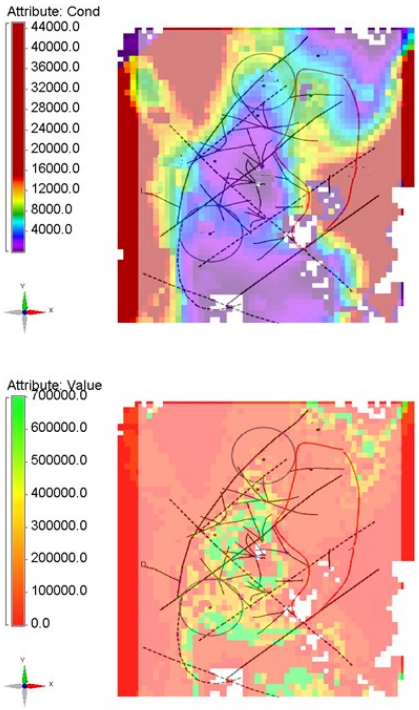

Figure 13: Plane View of field. Area within red solid line denotes location of possible future drilling campaign. a) conductance of clay cap interpreted with a 0.10 S/m threshold. b) resulting value ($) for each conductance bin (vj) calculated using posterior in Figure 11.

4. CONCLUSIONS

VOI is used to determine whether a particular type of data is worth acquiring and thus, the VOI must be calculated before the intended data is collected. We use a calibrated data set (electrical conductivity model from MT collocated with steam flow measurements) to estimate the past performance of MT to delineate the boundaries of the clay cap. Therefore, we assume that this VOI will be used to decide whether or not to purchase 3D MT at an analog field site. Specifically, we estimated the reliability of the data to reveal the principal uncertainty to the decision (θ_i representing steam flow for our example). In turn, we described how the value of imperfect information could be calculated with this reliability. We use a hypothetical decision scenario of "to drill or not" to define the other drivers of VOI: the prior probability, the value outcomes of Table 1. These would need to be refined in order to use these VOI estimates to determine whether or not to purchase the information.

This study indicates that the different interpretations of the clay cap do not greatly impact the assessed VOI of the MT data. From a decision analysis stand point, the different $VOI_{imperfect}$'s are indistinguishable since they are within $10,000 of each other, and therefore, the decision to purchase MT or not would be the same given the result of these three $VOI_{imperfect}$'s

We also used VOI to aid in determining future drilling locations. These relied on the information posteriors calculated for each clay cap interpretation and the value outcomes of Table 1. Both demonstrated consistent patterns with the known fault traces. As expected, the value maps for the two calibrations that only relied on electrical conductivity thresholds were quite similar. The two value maps can be used by the operators and local experts to determine where they would want to drill their next well.

We appreciate funding from the DOE Geothermal Technologies Office. This research was performed under the auspices of the U.S. Department of Energy by Lawrence Livermore National Laboratory under Contract No. DE-AC52-07NA27344. LLNL-CONF-649076.

REFERENCES

Bratvold, R. B., Bickel, J. E., Risk, A., & Lohne, H. P. (2009). Value of Information in the Oil and Gas Industry : Past, Present, and Future. *Society of Peteroleum Engineers:Reservoir Evaluation & Engineering*, (August 2009), 11–14. doi:10.2118/110378-PA

Cumming, W. (2009). Geothermal resource conceptual models using surface exploration data. In *PROCEEDINGS, Thirty-Fourth Workshop on Geothermal Reservoir Engineering* (p. SGP–TR–187). Stanford, California.

Gunderson, R., Cumming, W., Astra, D., & Harvey, C. (2000). Analysis of smectite clays in geothermal drill cuttings by the methylene blue method : for well site geothermometry and resistivity sounding correlation. In *Proceedings World Geothermal Congress* (pp. 1175–1181).

Karlsdóttir, R., Vilhjálmsson, A., Árnason, K., & Beyene, A. (2012). *Þeistareykir Geothermal Area , Northern Iceland 3D Inversion of MT and TEM Data* (p. 173). Reykjavík. Retrieved from www.isor.is

Newman, G. A., & Alumbaugh, D. L. (2000). Three-dimensional magnetotelluric inversion using non-linear conjugate gradients. *Geophysical Journal International*, *140*(2), 410–424. doi:10.1046/j.1365-246x.2000.00007.x

Pratt, J., Raiffa, H., and Schlaifer, R. (1995). *Introduction To Statistical Decision Theory*. Cambridge, MA: The Massachusets Institute of Technology Press.

Rejeki, S., Rohrs, D., Nordquist, G., & Fitriyanto, A. (2010). Geologic Conceptual Model Update of the Darajat Geothermal Field , Indonesia. In *Proceedings World Geothermal Congress 2010* (pp. 25–29).

Trainor-Guitton, W. J., Ramirez, A., Ziagos, J., Mellors, R., & Roberts, J. (2013). An Initial Value Of Information (VOI) Framework For Geophysical Data Applied To The Exploration Of Geothermal Energy. In *PROCEEDINGS, Thirty-Eighth Workshop on Geothermal Reservoir Engineering, Stanford University, Stanford, California, February 11-13, 2013 SGP-TR-198*.

Trainor-Guitton, W. J., Ramirez, A., Ziagos, J., Mellors, R., Roberts, J., Juliusson, E., & Hoversten, G. M. (2013). Value of Spatial Information for Determining Geothermal Well Placement. *Geothermal Resources Council Transactions*, 1–18.

Ussher, G., Harvey, C., Johnstone, R., Anderson, E., & Zealand, N. (2000). Understanding the resistivities observed in geothermal systems. In *Proceedings World Geothermal Congress* (pp. 1915–1920).